# Supporting Information

## p-n Junction formation between CoPi and α-$Fe_2O_3$ layers enhances photo-charge separation and catalytic efficiencies for efficient visible light-driven water oxidation

Tomohiro Katsuki,[†] Zaki N. Zahran,[†, ‡*] Yuta Tsubonouchi,[†] Debraj Chandra,[†] Norihisa Hoshino[†] and Masayuki Yagi [†*].

[†]Department of Materials Science and Technology, Faculty of Engineering, Niigata University, 8050 Ikarashi-2, Niigata 9050-2181, Japan.

[‡]Faculty of Science, Tanta University, Tanta 5111, Egypt.

*Correspondence to: yagi@eng.niigata-u.ac.jp and znzahran@eng.niigata-u.ac.jp

**Contents**

**Table S1** Summary of PEC water oxidation performances of the state-of-the-art $\alpha$-$Fe_2O_3$/CoPi-based electrodes.[a)]

| Electrodes [b)] | Preparation Method | $E_{on}$ (V vs. RHE) | $E_{on}$ shift [c)] (mV) | $\eta_{sep}$ (%) [d)] | $\eta_{cat}$ (%) [d)] | $IPCE_{420}$ (%) [d)] | $ABPE_{max}$ (%) | Ref. |
|---|---|---|---|---|---|---|---|---|
| $\alpha$-$Fe_2O_3$/CoPi | Casting | 0.65 [e)] | 200 [e)] | 33 [f)] | 70 [f)] | 20 | 1.2 [f)] | This work |
| $Ga_2O_3$/$\alpha$-$Fe_2O_3$/CoPi | ALD | 0.60 [g)] | 100 [g)] | na | na | na | na | R1 |
| $\alpha$-$Fe_2O_3$-CF/CoPi | APCVD | 0.83 | 170 | na | na | 40 | na | R2 |
| $\alpha$-$Fe_2O_3$-CF/CoPi | APCVD | 0.80 | 100 | na | na | 8 | na | R3 |
| $\alpha$-$Fe_2O_3$-IO/CoPi | ED | 0.88 | 120 | na | na | 30 [h)] | na | R4 |
| $\alpha$-$Fe_2O_3$-NRs/N-CoPi | HT | 0.70 | 50 | na | na | 7 | na | R5 |
| $\alpha$-$Fe_2O_3$-CL/CoPi | HT | 0.80 | 110 | na | na | na | na | R6 |
| $\alpha$-$Fe_2O_3$-NRs/CoPi | HT | 0.81 | 110 | na | na | 12 | 0.12 | R7 |
| $\alpha$-$Fe_2O_3$-CL/CoPi-$NaBH_4$ | HT | 0.70 | 100 | na | na | na | 0.13 | R6 |
| $\alpha$-$Fe_2O_3$-PNs/CoPi | HT | 0.68 [i)] | 160 [i)] | 17 [i)] | 90 [i)] | na | na | R8 |
| $\alpha$-$Fe_2O_3$-NRs/CoPi | HT | 0.80 | ~200 | na | 80 | 20 | 0.21 | R9 |
| Co-Pi/$CaFe_2O_3$/α-$Fe_2O_3$ BNRs | APCVD | 0.64 | 80 | na | na | na | na | R10 |

[a)] Measured in a 1.0 M NaOH (pH 14.0) electrolyte solution, under 1 sun AM 1.5G, ALD: atomic layer deposition, na: not available, CF: cauliflower, APCVD: atmospheric pressure chemical vapor deposition, IO: inverse opal, ED: electrochemical deposition, NRs: nanorods, N-CoPi: nitrogen doped CoPi, HT: hydrothermal, CL: coralline, PNs: porous nanorods, BNRs: branched nanorods, [b)] coated on basal FTO electrodes, [c)] defined as the $E_{on}$ difference between the $\alpha$-$Fe_2O_3$ and $\alpha$-$Fe_2O_3$/CoPi electrodes, [d)] at 1.23 V vs. RHE, [e)] Xenon lamp (> 420 nm, 100 mW $cm^{-2}$), [f)] monoclinic light (420 nm, 7.06 mW $cm^{-2}$) from LED, [g)] 1.0 M KOH with HCl as supporting, [h)]at 0.5 V vs. Ag/AgCl (1.53 V vs RHE), [i)] 0.1 M KOH (pH 12.6)

**References:**


R1 O. Zandi and T. W. Hamann, *Journal of Physical Chemistry Letters*, 2014, **5**, 1522–1526.

R2 D. K. Zhong, M. Cornuz, K. Sivula, M. Grätzel and D. R. Gamelin, *Energy Environ Sci*, 2011, **4**, 1759–1764.

R3 D. K. Zhong, J. Sun, H. Inumaru and D. R. Gamelin, *J Am Chem Soc*, 2009, **131**, 6086–6087.

R4 X. Shi, K. Zhang and J. H. Park, *Int J Hydrogen Energy*, 2013, **38**, 12725–12732.

R5 H. Lee, K. H. Kim, W. H. Choi, B. C. Moon, H. J. Kong and J. K. Kang, *ACS Appl Mater Interfaces*, 2019, **11**, 44366–44374.

R6 J. Xiao, L. Fan, F. Zhao, Z. Huang, S. F. Zhou and G. Zhan, *J Catal*, 2020, **381**, 139–149.

R7 J. Xiao, L. Fan, Z. Huang, J. Zhong, F. Zhao, K. Xu, S. F. Zhou and G. Zhan, *Chinese Journal of Catalysis*, 2020, **41**, 1761–1771.

R8 G. Liu, N. Li, Y. Zhao, M. Wang, R. Yao, F. Zhao, Y. Wu and J. Li, *ACS Sustain Chem Eng*, 2019, **7**, 11377–11385.

R9 T. T. Li, Q. Zhou, J. Qian, Y. Hu and Y. Q. Zheng, *Electrochim Acta*, 2019, **307**, 92–99.

R10 D. Chen, Z. Liu, Z. Guo, M. Ruan and W. Yan, *ChemSusChem*, 2019, **12**, 3286–3295.

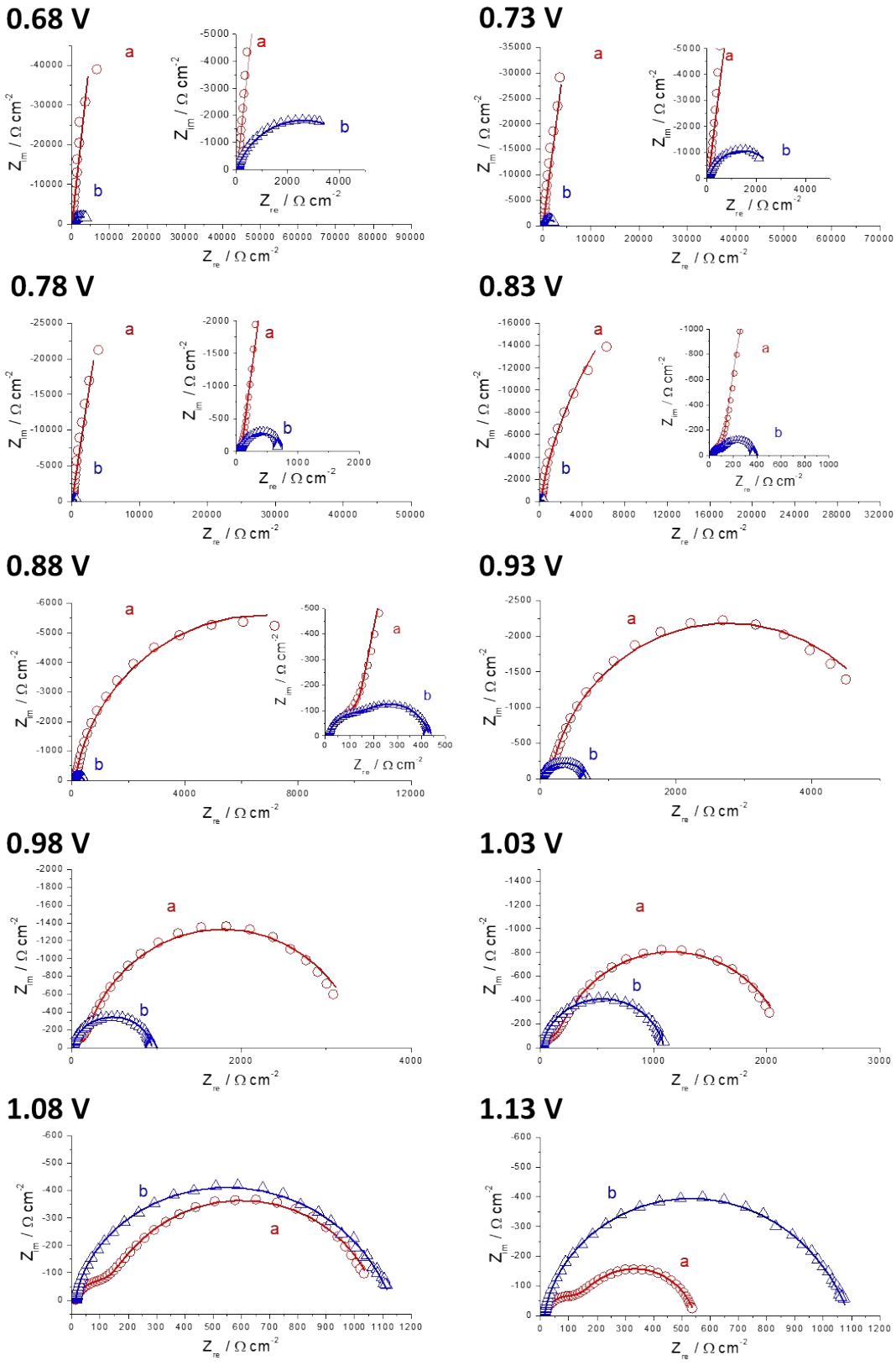


**Figure S1.** Nyquist plots and fitting curves using an equivalent circuit (inset of Figure 7A) for (a) $\alpha$-$Fe_2O_3$ and (b) $\alpha$-$Fe_2O_3$/CoPi electrodes in a 1.0 M NaOH solution (pH 14.0) at frequencies from 100 mHz to 20 kHz at different potentials ($E$) of 0.68-1.53 V vs RHE (-0.35 – 0.50 V vs Ag/AgCl) under visible light irradiation (>420 nm, 100 mW $cm^{-2}$).

Figure S2 continued

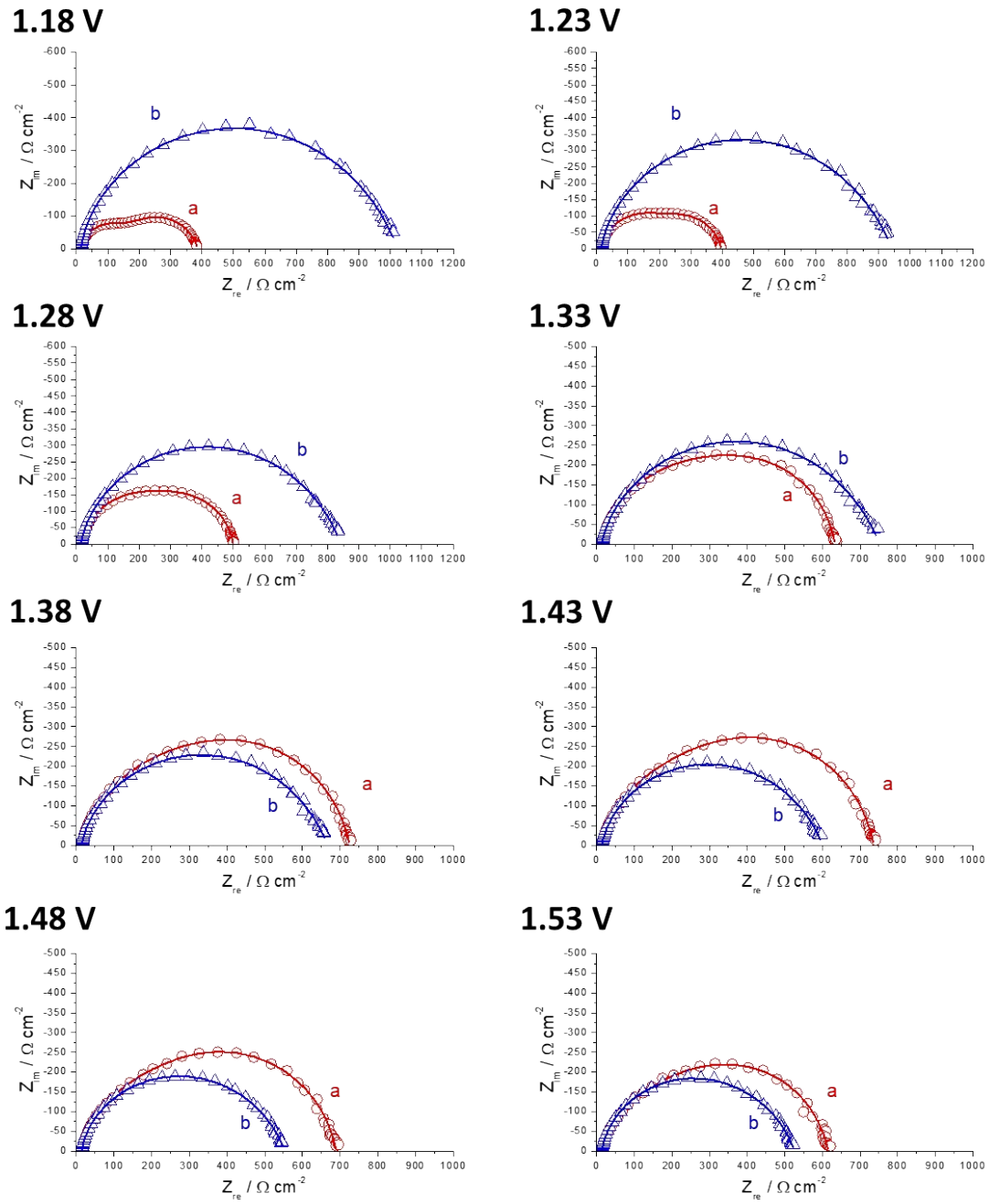

**Table S2** Fitting parameters of components of $R_{sol}$, $R_{ct}$ and CPE analyzed in the equivalent circuit (inset of Figure 7A) at different potentials ($E$) for $\alpha$-$Fe_2O_3$ and $\alpha$-$Fe_2O_3$/CoPi electrodes.

| **$\alpha$-$Fe_2O_3$ electrode** | | High frequency | | | Low frequency | | |
|---|---|---|---|---|---|---|---|
| | | CPE$^{bulk}$ | | | CPE$^{surf}$ | | |
| $E$ vs RHE | $R_{sol}$ [Ω] | $R_{ct}^{bulk}$ [Ω] | $T_{CPE}^{bulk}$ [μF s$^{(p-1)}$] | $p$ | $R_{ct}^{surf}$ [Ω] | $T_{CPE}^{surf}$ [μF s$^{(p-1)}$] | $p$ |
| 0.68 | 14.5 | 132 | 27.7 | 0.921 | $5.17\times10^{13}$ | 13.4 | 0.942 |
| 0.73 | 14.4 | 193 | 34.7 | 0.888 | $6.07\times10^{9}$ | 20.3 | 0.962 |
| 0.78 | 14.1 | 201 | 42.5 | 0.851 | $7.82\times10^{6}$ | 33.5 | 0.966 |
| 0.83 | 13.7 | 221 | 51.0 | 0.817 | $7.77\times10^{4}$ | 48.9 | 0.965 |
| 0.88 | 13.5 | 250 | 50.2 | 0.809 | $1.33\times10^{4}$ | 62.0 | 0.950 |
| 0.93 | 13.4 | 298 | 47.7 | 0.808 | 5120 | 64.9 | 0.929 |
| 0.98 | 13.3 | 302 | 46.1 | 0.806 | 3120 | 69.8 | 0.901 |
| 1.03 | 13.3 | 223 | 39.7 | 0.816 | 1950 | 103 | 0.860 |
| 1.08 | 13.4 | 161 | 29.7 | 0.843 | 906 | 180 | 0.825 |
| 1.13 | 13.6 | 148 | 23.4 | 0.864 | 385 | 268 | 0.807 |
| 1.18 | 13.6 | 177 | 21.3 | 0.872 | 195 | 290 | 0.822 |
| 1.23 | 13.7 | 252 | 21.2 | 0.870 | 131 | 232 | 0.878 |
| 1.28 | 13.7 | 368 | 21.2 | 0.867 | 118 | 144 | 0.947 |
| 1.33 | 13.7 | 499 | 21.7 | 0.862 | 121 | 89.2 | 1.00 |
| 1.38 | 13.6 | 564 | 22.1 | 0.857 | 147 | 58.9 | 1.00 |
| 1.43 | 13.6 | 535 | 21.5 | 0.857 | 188 | 41.7 | 0.997 |
| 1.48 | 13.6 | 477 | 21.0 | 0.857 | 199 | 44.8 | 0.962 |
| 1.53 | 13.6 | 411 | 20.2 | 0.859 | 191 | 51.1 | 0.930 |

| **$\alpha$-$Fe_2O_3$/CoPi electrode** | | High frequency | | | Low frequency | | |
|---|---|---|---|---|---|---|---|
| | | | CPE$^{bulk}$ | | | CPE$^{surf}$ | |
| $E$ vs RHE | $R_{sol}$ [Ω] | $R_{ct}^{bulk}$ [Ω] | $T_{CPE}^{bulk}$ [μF s$^{(p-1)}$] | $p$ | $R_{ct}^{surf}$ [Ω] | $T_{CPE}^{surf}$ [μF s$^{(p-1)}$] | $p$ |
| 0.68 | 13.6 | 96.4 | 62.3 | 0.846 | 5100 | 92.7 | 0.735 |
| 0.73 | 13.3 | 91.9 | 67.5 | 0.821 | 2730 | 153 | 0.831 |
| 0.78 | 13.4 | 76.1 | 47.7 | 0.851 | 654 | 225 | 0.863 |
| 0.83 | 13.5 | 97.8 | 37.0 | 0.875 | 270 | 279 | 0.851 |
| 0.88 | 13.6 | 186 | 30.4 | 0.895 | 232 | 251 | 0.838 |
| 0.93 | 13.7 | 385 | 26.2 | 0.909 | 269 | 187 | 0.829 |
| 0.98 | 13.8 | 631 | 24.4 | 0.914 | 301 | 154 | 0.830 |
| 1.03 | 13.8 | 740 | 24.0 | 0.914 | 340 | 153 | 0.760 |
| 1.08 | 13.8 | 708 | 24.3 | 0.911 | 409 | 191 | 0.646 |
| 1.13 | 13.7 | 676 | 25.7 | 0.905 | 404 | 193 | 0.634 |
| 1.18 | 13.7 | 594 | 27.0 | 0.899 | 417 | 167 | 0.628 |
| 1.23 | 13.7 | 511 | 28.8 | 0.893 | 420 | 167 | 0.603 |
| 1.28 | 13.7 | 451 | 30.3 | 0.888 | 380 | 162 | 0.623 |
| 1.33 | 13.7 | 390 | 30.8 | 0.887 | 349 | 168 | 0.629 |
| 1.38 | 13.6 | 367 | 31.4 | 0.883 | 287 | 199 | 0.635 |
| 1.43 | 13.6 | 356 | 30.5 | 0.884 | 232 | 248 | 0.638 |
| 1.48 | 13.6 | 347 | 28.0 | 0.888 | 192 | 274 | 0.658 |
| 1.53 | 13.6 | 353 | 25.0 | 0.896 | 160 | 313 | 0.662 |